Relationship between the Structure and Slow Crack Growth in Blends of High-Density Polyethylene and Model Copolymers

N. Brown* and Z. Zhou

Department of Materials Science and Engineering, University of Pennsylvania, Philadelphia, Pennsylvania 19104-6272

Received July 11, 1994; Revised Manuscript Received January 4, 1995[®]

ABSTRACT: The resistance to slow crack growth (SCG) was investigated in binary blends of high-density polyethylene (HDPE) and a model monodispersed ethylene–butene copolymer. The results were correlated with the morphological structure of the blends by a simple quantitative theory. The time to failure (t_f) depended on crystallinity, crystal thickness, and most importantly the intrinsic resistance to SCG of the crystal network as determined by the density and branching of its tie molecule. t_f was measured from 30 to 80 °C. At lower testing temperatures from 30 to 60 °C, the blend with the thinnest crystals had the longest t_f. However, at the higher temperature of 80 °C, the blend with the thinnest crystals became weaker relative to the blends with thicker crystals. The activation energy increased as the crystal thickness decreased.

Introduction

In a previous paper by Zhou, Brown, and Crist,[1] slow crack growth (SCG) was measured at 42 °C in the same blends used in the present investigation. These results could be explained qualitatively in terms of the morphology of each blend. In this paper, a more quantitative and simple explanation of the results is presented by constructing a schematic of the morphology of each blend drawn to scale and by using a simple quantitative theory. The effect of temperature on SCG was also measured. The key to understanding the effect of temperature is based on the work of Lu *et al.*[2] which showed that the amount of decrease in resistance to SCG with increasing temperature was greatest when the crystal thickness was least.

Experimental Section

The binary blends consist of a commercial high-density polyethylene (HDPE) with a small concentration of a model ethylene–butene random copolymer. The components of each blend and the blends themselves are characterized in Tables 1 and 2. The copolymers are monodispersed with about the same molecular weight and were produced from hydrogenated polybutadiene. The branch density of the copolymers varied from 15 to 117 branches/1000C. Previous papers by Crist and co-workers[1,3–5] describe in detail the molecular structure, the phase behavior, the preparation of the blends, and their mechanical properties. In particular, they found B1 and B2 formed one phase in the liquid state and probably the copolymer cocrystallized with unbranched chains. They also observed that in B3 the copolymer was phase separated and formed ~1 μm amorphous droplets in the solid.

SCG was measured under plane strain conditions with a constant stress of 3 MPa and a notch depth of 1.4 mm with a single edge notch specimen. The stress intensity, $K = 0.37$ MPa m$^{1/2}$. The geometry of the test specimen is shown in Figure 1. The tests were done at 30, 42, 60, and 80 °C. The crack opening displacement (COD) was measured as a function of time by looking into the root of the notch with an optical microscope, and typical curves of COD vs t are shown in Figure 2. The essential data for the measurement of SCG is the total time to failure. Previous work by Brown *et al.*[6] showed that the resistance to SCG of a resin can also be represented equally well by the time to initiate fracture as by the time for complete fracture (t_f).

Results

The times to failure, t_f, for each blend are shown in Table 3. The blends will be designated as B0, B1, B2, and B3 in order of increasing branch density of the copolymer. It is to be noted that resistance to SCG, as measured by t_f, follows the sequence B2 > B1 > B0 > B3 at low temperatures. As the temperature increases, t_f generally decreases, but the relative values of t_f change so that at 80 °C the sequence of t_f becomes B1 > B0 > B2 > B3. t_f is plotted against $1/T$ in Figure 3 where the slopes give activation energies which vary from 121 to 147 kJ/mol (Table 3).

Models of the morphology of each blend are shown in Figure 4. The models of the morphology are based on data as given below. The crystallinity is obtained from the density of each blend in accordance with the equation:

$$X = \frac{\varrho - \varrho_A}{\varrho_c - \varrho_A} \qquad (1)$$

where $\varrho_A = 860$ and $\varrho_c = 1000$ kg/m^3. The model is simplified by assuming that there are two populations of crystal sizes and that the volume of crystal for each size is in proportion to the concentration of the two components. The thicknesses of the crystals in the blend from the HDPE component are assumed to be equal to that for pure HDPE. The thickness of the crystals from the copolymer is assumed to be inversely proportional to the average branch density. The absolute value of the crystal thickness of the HDPE component was calculated from the DSC curves obtained in the previous paper by Zhou, Brown, and Crist[1] and by using the equation that crystal thickness

$$l_c = \frac{0.626 \times 414}{414 - T_m} \text{nm} \qquad (2)$$

as proposed by Illers and Hendus.[7] Since the melting point T_m for B0 is 135 °C and those for the copolymers in B1 and B2 are 110 and 75 °C, the corresponding crystal thicknesses are $l_c(B0) = 43$ nm, $l_c(B1) = 8$ nm, and $l_c(B2) = 4$ nm, respectively. Assuming that for the copolymers the average crystal thickness is equal to the average branch spacing, $l(B1) = 8.5$ nm and $l(B2) = 2.1$ nm which are close to the values obtained from eq 2.

Table 1. Polymer Characteristics of Components in the Blend

component	branches/ 1000C	M_w	M_w/M_n	ϱ (kg/m^3)	X (%)	ADB^a (nm)	crystal^b thickness (nm)	T_m (°C)
HDPE	0	164 000	11	~970	~80		43	135
HPB15	15	119 000	1.1	905	44	8.5	8	110
HPB61	61	109 000	1.1	890	29	2.1	4	75
HPB117	117	122 000	1.2	860	0	1.1		

^{a} ADB: average distance between branches. ^{b} Calculated from $l_c = 0.626 \times 414/(414 - T_m)$ (Illers and Hendus[7]).

Table 2. Characteristics of Blends

blend	composition	av br 1000C	melt phase	l_c (nm)	T_m^a (°C)	ϱ^b (kg/m^3)	X^c (%)
B0	PE	0	one	43	135.0	972	80
B1	PE/HPB15 (10%)	1.5	one	37	133.9	965	73
B2	PE/HPB61 (10%)	5.5	one	25	130.6	960	70
B3	PE/HPB117 (5%)	4.8	two	39	134.4	965	75

^{a} DSC results at the heating rate of 5 °C/min for T_m. ^{b} For slowly cooled samples from the density gradient column. ^{c} For slowly cooled samples measured from DSC curves. 0.5 °C/min, heat of fusion = 289 J/mol.
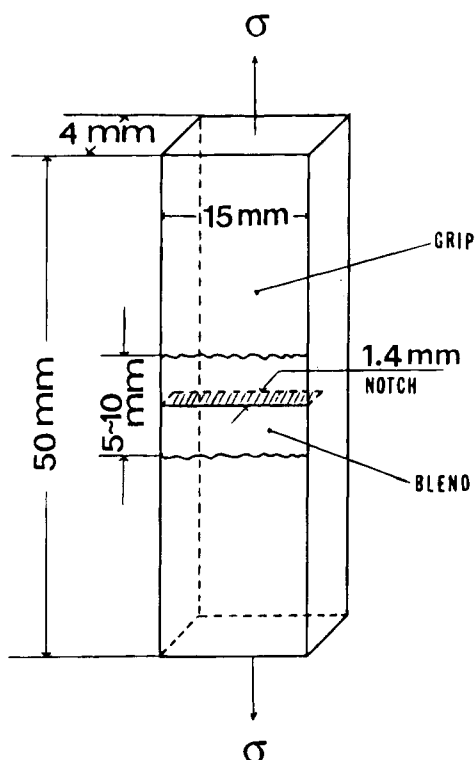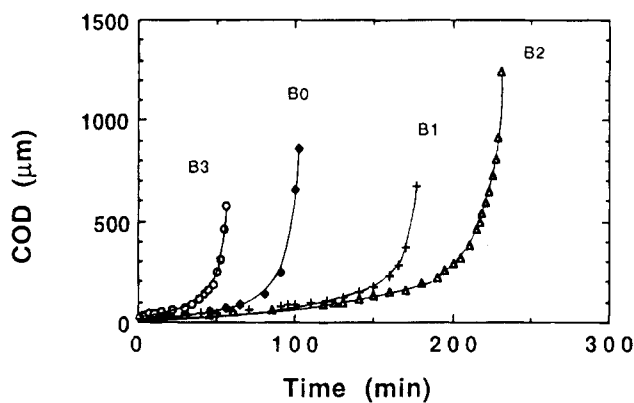

Figure 1. Geometry of the test specimen.

(a)

(b)

Figure 2. Crack opening displacement versus time for each blend: 3 MPa, notch depth 1.40 mm. (a) 60 °C; (b) 80 °C.

Table 3. Slow Crack Growth Behavior

material	time to failure (min)				activation energy (kJ/mol)
	30 °C	42 °C	60 °C	80 °C	
B0	7 538	1000	100	7.4	121
B1	12 760	1853	180	9.7	125
B2	25 042	3699	209	7.1	147
B3	4 318	523	55	4.3	121

The copolymer in B3 does not crystallize as indicated by its density of 860 kg/m^3 and by the formation of rubber particles in the amorphous phase as shown in the microscopic examination by Rhee and Crist.[5]
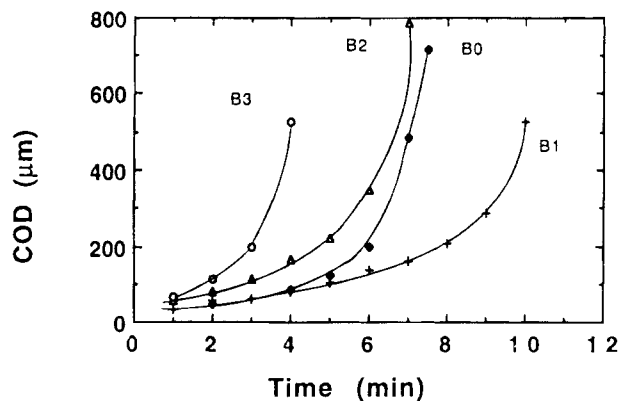
The density of tie molecules in each of the crystalline regions is estimated from the theory of Huang and Brown[8] where the probability of forming a tie molecule is given by:

$$P = \frac{\int_L^\infty r^2 \exp(-b^2 r^2)\, dr}{3\int_0^\infty r^2 \exp(-b^2 r^2)\, dr} \qquad (3)$$

where r = end-to-end distance of the random coil, $b^2 = (3/2)\bar{r}^2$ where $\bar{r}$ is the root mean square of the end-to-end distance, and $L = 2l_c + l_a$ where l_c = crystal thickness and l_a = thickness of the amorphous layer. The factor 3 in the denominator of eq 3 is based on the

geometry of a lamella crystal since a tie molecule forms along one of the crystal dimensions. The value of $\bar{r}$ depends on the molecular weight and is given by $\bar{r} = (Dnl^2)^{1/2}$ where $D = 6.8$ for PE and the link length $l = 0.153$ nm and n is the number of links. The value of l_a is obtained from the equation:

$$\frac{l_c}{l_c + 0.86 l_a} = X$$

Values of X are in Table 1 as are M_ws for each component of the blends.

All the quantities are available for calculating the probability of forming a tie molecule, P, from eq 3. Table 4 contains the parameters for producing the quantita-
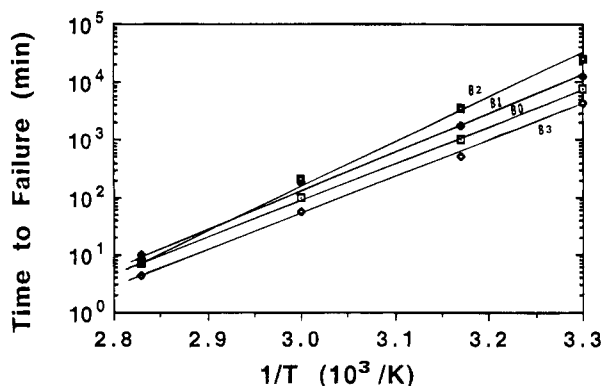
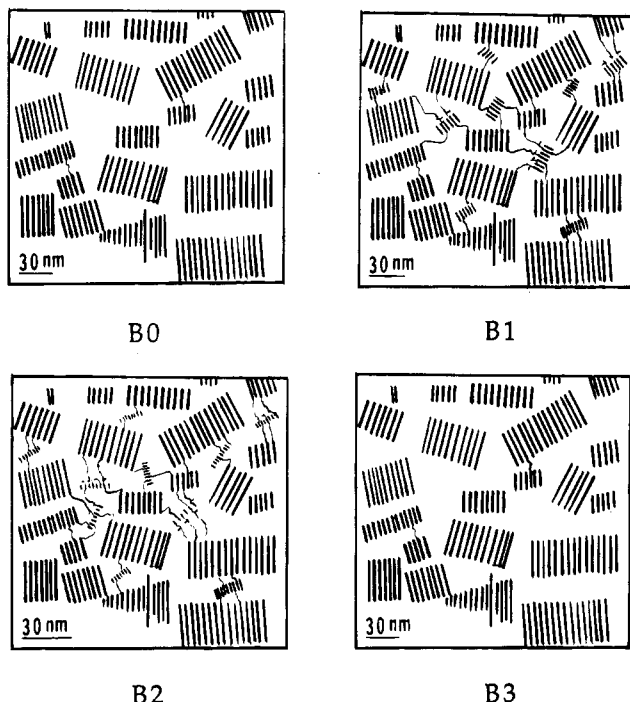**Figure 3.** Time to failure versus $1/T$ for each blend.

Figure 4. Morphology of the blends drawn to scale. The white areas represent the amorphous regions. The lamella crystals are oriented in accordance with the oriented fibrils in the craze. The direction of the applied stress is vertical. The B3 blend contains 1 μm droplets of the segregated copolymer, but the droplets are not shown in this scale because they represent 5% of the material.

Table 4

blend	% copolymer	crystal-linity	crystal thickness (nm)		amorphous layer (nm)	tie molecule[a]
			HDPE	co-polymer		
B0	0	80	43		11	6×10^{-4}
B1	10	73	37	8	13	5×10^{-2}
B2	10	70	5	4	24	7×10^{-2}
B3	5	75	39		13	6×10^{-4}

[a] Probability of forming a tie molecule.

tive schematics of the morphology shown in Figure 4. The guidance as to how the fine crystals of the copolymer may be dispersed relative to the coarse crystals of the homopolymer was offered by the electron micrographs of the lamella structure taken by Bassett[9] where the fine crystals are dispersed between the coarse crystals. It is important to note that the white area in Figure 4 represents the liquidlike amorphous region that offers no resistance to SCG. The structure of B0 is practically the same as that of B3 because the

copolymer is completely segregated into 1 μm amorphous droplets. For blends B1 and B3 the tie molecules are mostly between the small and large crystals. It should be remembered that these illustrations are simplifications because the actual structure consists of a distribution of crystal thicknesses as indicated by DSC data.

Fracture occurs by a breakdown of the fibrils of the craze which occurs at the root of the notch. The diameter of the fibrils is on the order of 10^2-10^3 nm, which is much larger than the crystal dimensions; thus, the schematics as represented in Figure 4 are representative of the overall fibril morphology.

It is desirable to mathematically describe the relationship between t_f and the structure. It should be realized that the following theory is a rough first approximation of a very complex phenomenon. However, this theory permits us to clearly focus on the important structural parameters that determine t_f. It is assumed that the resistance to SCG of a blend depends on the following parameters: (1) degree of crystallinity; (2) the relative proportion of the number of coarse and fine crystals; (3) the intrinsic resistances to SCG of the fine and coarse crystal networks as determined by the density and branching of their tie molecule. A unit volume of fine crystals has a greater strength than a unit volume of coarse crystals, because the number per unit volume which varies as $1/l_c$ is greater. Also, the intrinsic strength of the network containing fine crystals is greater because they contain more tie molecules and they are highly branched. The above assumptions can now be represented by the following theoretical equation where the resistance to SCG is represented by:

$$t_f = CX\left(\frac{A_c}{l_c}\right) + (1 - C)X\frac{A_h}{l_h} \tag{4}$$

where C is the concentration of copolymer, X is the crystallinity of the blend, l_c and l_h are the thicknesses of the copolymer and homopolymer crystals, and A_c and A_h are the intrinsic strengths of the copolymer and homopolymer crystals. The density of a blend is proportional to the concentration of each component, and therefore it is expected that the crystallinity is also proportional to the concentration where

$$X = CX_c + (1 - C)X_h \tag{5}$$

X_c and X_h are the crystallinities of each component, copolymer and homopolymer, respectively. When eqs 4 and 5 are combined:

$$t_f = C[CX_c + (1 - C)X_h]\frac{A_c}{l_c} +$$
$$(1 - C)[CX_c + (1 - C)X_h]\frac{A_h}{l_h} \tag{6}$$

Equation 6 will now be applied to the experimental data as presented in Figure 5 where $t_f/t_f(c=0)$ is plotted against composition for the present blends and for a blend of HDPE with a copolymer with 4.5 branches/1000C as determined by Zhou, Lu, and Brown.[10] It is of interest to compare the experimental value of the initial slope of t_f vs C and the theoretical value obtained by differentiating eq 6.
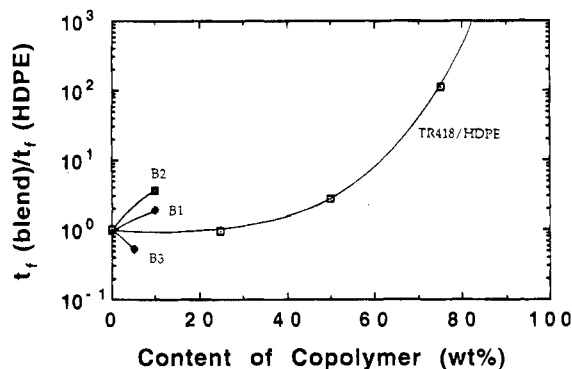
Figure 5. Lifetime of a blend divided by the lifetime of the homopolymer versus composition at 42 °C.

$$\frac{1}{t_f(c=0)}\frac{dt_f}{dc}(c=0) = \frac{A_c/l_c}{A_h/l_h} + \frac{X_c - 2X_h}{X_h} \qquad (7)$$

In Table 5 values of the intrinsic resistance to SCG of the copolymer relative to that of the homopolymer matrix, $(A_c/l_c)/(A_h/l_h)$, for each blend have been derived from the experimental data in Figure 5 and the theoretical equation 7. The experimental observations are in complete accord with theory in that the initial slope in Figure 5 increases with $(A_c/l_c)/(A_h/l_h)$, the intrinsic resistance to SCG. A_c and A_h are functions of temperature and branch density. For the case of blend B3, theory suggests that amorphous particles produced by the copolymer primarily weaken the blend by reducing the crystallinity.

The theoretical equation (6) is expected to be valid for concentrations of the copolymer less than 50%. The experimental data for the blend with 4.5 branches/1000C exhibit an extremely rapid increase in t_f for concentrations of the copolymer greater than 50%. It has been suggested by Zhou, Lu, and Brown[8] that this rapid increase occurs when the strong component becomes the matrix and forms a continuous crystalline—tie molecule network. Equation 6 should apply when the copolymer crystals occur as islands within the homopolymer matrix.

There is, however, another important factor that is not included in the theory. As the crystallinity of the blend decreases, the resin becomes more compliant so that the original sharp notch becomes blunter for a given applied stress. The blunting of the notch decreases the stress concentration so that t_f tends to increase.

The changes in t_f with respect to an increase in the testing temperature is shown in Table 3. There is a general exponential decrease in t_f with increasing temperature because the process of chain sliding that occurs during disentanglement is a thermally activated process. In addition, t_f decreases because the crystals that anchor the tie molecules soften with increasing temperature. This softening is associated with the α transition and becomes appreciable above 60 °C. The fact that the softening temperature increases as the crystal thickness increases was pointed out by Lu, McGhie, and Brown,[2] who measured the effect of testing temperatures on SCG, and by Boyd,[11] Mansfield and Boyd,[12] and Popli et al.[13] based on dynamic mechanical measurements. Whereas below 60 °C, blend B2 is the strongest resin, at 80 °C it is weaker than B0. At 80 °C B1 is less strong relative to B0. The reason is simply that crystal thickness ranks in the order B0 >

Table 5[a]

blend	copolymer branch	density ϱ_c	ϱ_h	$(X_c - 2X_h)/X_h{}^b$	$\dfrac{dt_f}{dc}/t_f(c=0)$	$\dfrac{A_c/l_c{}^c}{A_h/l_n}$
TR418/ HDPE	4.5	945	973	−1.22	1.5	2.7
B1	15	905	970	−1.56	8.5	10
B2	61	890	970	−1.70	26	28
B3	117	860	970	−2	−9.1	−7.1

[a] At 42 °C. [b] Crystallinities were calculated from the densities using eq 1. [c] Equals [initial slope of Figure 5 − $(X_c - 2X_h)/X_h$.]

B1 > B2. The ratio of $t_f(B0)/t_f(B3)$ is essentially independent of temperature because the crystal thickness is the same in both blends.

Probably the differences in activation energy exhibited by the blends (Table 3) are caused by the differences in the rate of crystal softening as the temperature is increased. Thus, the activation energy is expected to increase as the crystal thickness decreases.

In order to physically appreciate the effect of morphology on the resistance to slow crack growth, observe Figure 4 and visualize the effect of a constant tensile stress applied in the vertical direction. The applied stress is less than half the yield point so that only chain disentanglement and not scission is most probable. Only the tie molecules hold the crystals together. The load produced by the stress is supported by the tie molecules. The amorphous region in white offers no resistance because the test is well above T_g. The slow crack growth process consists of the pulling of the crystals by the tie molecules. The greater the number of tie molecules, the smaller the force exerted on the crystal by each tie molecule. The exact mechanism by which the tie molecules disengage from the crystals is not known. Probably the tie molecules tend to shred the crystals. The intrinsic strength of the crystals is important. Thus, as the temperature is raised, the crystal softening occurs as is generally attributed to the α transition. The thinner crystals soften more readily than the thicker ones. The fact that t_f at 80 °C for B2 is slightly less than that for B0 indicates that the crystals from the copolymer offers no resistance to SCG and, in addition, the volume of thick crystals is less.

In the case of blend B3, the copolymer is simply part of the amorphous region and thus decreases the overall crystallinity but has practically no effect on the thickness of the crystals. It is interesting to note that the presence of the copolymer in B3 reduces the crystallinity by 5% but decreases the time to failure by about 50%. Probably, the copolymer reduces the probability of forming a tie molecule by increasing the long period.

The magnitude of the changes in t_f for the blends with copolymer concentrations of 10% or less is small compared to the maximum strength that is possible at much higher concentrations. The findings for this investigation are made possible because the test method is very sensitive to differences in the morphological and molecular structure of the blend and because t_f can be measured with a high degree of precision.

References and Notes

(1) Zhou, Z.; Brown, N.; Crist, B. *J. Polym. Sci.*, in press.
(2) Lu, X.; McGhie, A.; Brown, N. *J. Polym. Sci., Part B: Phys.* **1992**, *30*, 1207.
(3) Howard, P. R.; Crist, B. *J. Polym. Sci., Part B: Phys.* **1989**, *27*, 2269.
(4) Krigas, T.; Carello, J. M.; Struglinski, M. J.; Crist, B.; Graessley, W. W.; Schilling, F. C. *J. Polym. Sci., Part B: Phys.* **1985**, *23*, 509.
(5) Rhee, J.; Crist, B. *J. Polym. Sci., Part B: Phys.* **1994**, *32*, 159.
(6) Brown, N.; Lu, X.; Huang, Y.; Qian, R. *Makromol. Chem., Macromol. Symp.* **1991**, *41*, 55.
(7) Illers, V. K. H.; Hendus, H. *Makromol. Chem.* **1968**, *113*, 1.
(8) Huang, Y.; Brown, N. *J. Polym. Sci., Part B:* Phys. **1991**, *29*, 129.
(9) Bassett, D. C. *Principles of Polymer Morphology*; Cambridge University Press: New York, 1981; Figure 5, p 121.
(10) Zhou, Z.; Lu, X.; Brown, N. *Polymer* **1993**, *34*, 2520.
(11) Boyd, R. H. *Polymer* **1985**, *26*, 323.
(12) Mansfield, M.; Boyd, R. H. *J. Polym. Sci., Polym. Phys.* **1978**, *16*, 1227.
(13) Popli, M.; Glotin, M.; Mandelkern, L.; Benson, R. S. *J. Polym. Sci., Phys.* **1984**, *22*, 407.